Telomere-based crisis: functional differences between telomerase activation and ALT in tumor progression

Sandy Chang,[1,3,4] Christine M. Khoo,[1,2] Maria L. Naylor,[1,2] Richard S. Maser,[1,2] and Ronald A. DePinho[1,2,5]

[1]Department of Medical Oncology, Dana Farber Cancer Institute, Boston, Massachusetts 02115 USA; [2]Department of Medicine and Genetics, Harvard Medical School, Boston, Massachusetts 02115 USA; [3]Department of Pathology, Brigham and Women's Hospital, Boston, Massachusetts 02115 USA

Telomerase activation is a common feature of most advanced human cancers and is postulated to restore genomic stability to a level permissive for cell viability and tumor progression. Here, we used genetically defined transformed mouse embryonic fibroblast (MEF) cultures derived from late generation *mTerc*$^{-/-}$ *Ink4a/Arf*$^{-/-}$ mice to explore more directly how telomere-based crisis relates to the evolution of cancer cell genomes and to tumor biology. An exhaustive serial analysis of cytogenetic profiles over extensive passage in culture revealed that the emergence of chromosomal fusions (including dicentrics) coincided with onset of deletions and complex nonreciprocal translocations (NRTs), whereas *mTerc*-transduced cultures maintained intact chromosomes and stable genomes. Despite a high degree of telomere dysfunction and genomic instability, transformed late passage *mTerc*$^{-/-}$ *Ink4a/Arf*$^{-/-}$ cultures retained the capacity to form subcutaneous tumors in immunocompromised mice. However, even moderate levels of telomere dysfunction completely abrogated the capacity of these cells to form lung metastases after tail-vein injection, whereas *mTerc* reconstitution alone conferred robust metastatic activity in these cells. Finally, serial subcutaneous tumor formation using late passage transformed *mTerc*$^{-/-}$ *Ink4a/Arf*$^{-/-}$ cultures revealed clear evidence of telomerase-independent alternative lengthening of telomeres (ALT). Significantly, despite a marked increase in telomere reserve, cells derived from the ALT+ subcutaneous tumors were unable to generate lung metastases, indicating in vivo functional differences in these principal mechanisms of telomere maintenance. Together, these results are consistent with the model that although telomere dysfunction provokes chromosomal aberrations that initiate carcinogenesis, telomerase-mediated telomere maintenance enables such initiated cells to efficiently achieve a fully malignant endpoint, including metastasis.

[*Keywords*: Telomere; telomerase; metastasis; ALT (alternative lengthening of telomeres); chromosomal instability; SKY]

Supplemental material is available at http://www.genesdev.org.

Received October 17, 2002; revised version accepted November 6, 2002.

Tumor formation represents the phenotypic endpoint of a mutational process that endows cells with a critical threshold of cancer-relevant genetic lesions. From a cytogenetic standpoint, epithelial neoplasms or carcinomas fall into one of two major classes—the first possessing microsatellite instability with retention of grossly normal karyotypes, and the second presenting with markedly altered chromosomal counts and structure. These two classes have been operationally defined as "microsatellite instability neoplasias" and "chromosomal instability neoplasias" (MIN and CIN), respectively (for review, see Lengauer et al. 1998). The molecular mechanism underlying MIN is clearly related to defective DNA mismatch repair. The basis for CIN is less well understood, although defects in mitotic checkpoint, nonhomologous end-joining, and DNA replication, as well as increased oxidative stress and telomere dysfunction, have emerged as prime candidates (Elledge 1996; Bohr and Dianov 1999; Shen et al. 2000; O'Driscoll et al. 2001; O'Hagan et al. 2002). Because the vast majority of human cancer genomes are of the CIN-type, significant effort has been directed toward understanding the contribution of these and other mechanisms to genomic instability.

The link between telomere function and genome sta-

[4]Present address: Department of Molecular Genetics, M.D. Anderson Cancer Center, 1515 Holcombe Blvd, Houston, TX 77030, USA.
[5]Corresponding author.
E-MAIL ron_depinho@dfci.harvard.edu; FAX (617) 632-6069.
Article and publication are at http://www.genesdev.org/cgi/doi/10.1101/gad.1029903.

bility first came to light in the work of McClintock (1941), from which emerged the concept that telomeres cap and maintain chromosome structural integrity. Telomeres consist of G-rich simple-repeat sequences at chromosomal termini and serve to protect natural DNA ends from being recognized as double-stranded breaks that would otherwise activate DNA damage checkpoint responses or participate in recombination events (Blackburn 2001). The synthesis and maintenance of telomeres are mediated by telomerase, a specialized ribonucleoprotein complex that includes an RNA template (*Terc*) and a reverse transcriptase catalytic subunit (TERT; for review, see Greider 1996). In the absence of telomerase, each round of DNA replication is accompanied by telomere shortening owing to the failure of DNA polymerase to synthesize fully the extreme terminus of the lagging DNA strand.

In human cell-culture model systems, the biological and genomic consequences of telomere shortening have been well documented (Harley et al. 1990; Allsopp et al. 1992). Critical telomere attrition has been shown to cause replicative senescence via activation of the p53 and pRB tumor suppressor pathways (Wright and Shay 1992). Correspondingly, inactivation of p53 and pRB by antisense neutralization (Hara et al. 1991) or by viral oncoproteins (Shay et al. 1991) can extend replicative potential, driving further telomere erosion and culminating in a period of massive cell death and rampant chromosomal instability termed crisis (Counter et al. 1992). Virally transformed human cells escape crisis at extremely low frequencies (Shay et al. 1993), whereas those expressing hTERT readily escape senescence and are immortalized (Bodnar et al. 1998; Vaziri and Benchimol 1998). In addition, cells engineered to express SV40 small and large T antigen, activated RAS, and hTERT are readily transformed (Hahn et al. 1999a). Moreover, ~80% to 90% of human tumors possess telomerase activity, whereas the remainder maintains telomeres via a recombination-mediated process termed ALT (for alternative lengthening of telomeres; Kim et al. 1994; Bryan et al. 1997; Shay and Bacchetti 1997). Together, these observations support the view that cellular crisis provides a potent barrier to tumor development and, by extension, that telomere maintenance is an essential aspect of full malignant progression. That such telomere-related events occur in the evolution of primary human tumors has been inferred by (1) the shorter telomere lengths of tumors relative to normal tissue (de Lange et al. 1990; Hastie et al. 1990), (2) the presence of anaphase bridges during early tumor development (de Lange 1995; Gisselsson et al. 2000; Rudolph et al. 2000), and (3) the marked increase in telomerase activity with malignant progression (Kim et al. 1994; Shay and Bacchetti 1997; Tang et al. 1998; Yan et al. 1999).

The telomerase knockout mouse has provided insight into the complex interactions between telomere dynamics and tumor genesis and progression. In cancer-prone *Ink4a/Arf* mutant or Apc^{Min} mice and in a carcinogen-induced skin cancer model, telomere dysfunction results in a marked reduction in tumor incidence and prolonged survival (Greenberg et al. 1999; Gonzalez-Suarez et al. 2000; Rudolph et al. 2000). In contrast, in a *p53* mutant setting (distinguished from *Ink4a/Arf* and Apc^{Min} models by an attenuated DNA double-strand break checkpoint response), the cellular and organismal response to telomere dysfunction is reprogrammed into one of improved cellular proliferation and survival, accelerated tumorigenesis, and marked shift in tumor spectrum toward carcinomas (Chin et al. 1999; Artandi et al. 2000). Extensive cytogenetic analysis of primary cells and tumors derived from *p53* mutant mice possessing short dysfunctional telomeres has revealed an increased frequency of chromosomal fusions (Chin et al. 1999), emergence of marked aneuploidy and complex nonreciprocal translocations (NRTs; Artandi et al. 2000), and regional chromosomal amplifications and deletions (O'Hagan et al. 2002). On the basis of these findings, we have proposed that the classic breakage-fusion-bridge (BFB) process (McClintock 1941) provides a mechanism that enables would-be cancer cells to acquire the threshold of genetic gains and losses favorable to clonal outgrowth and tumor initiation and progression (for review, see Maser and DePinho 2002).

In this study, we make use of transformed mouse embryonic fibroblast (MEF) cultures derived from late generation $mTerc^{-/-}$ $Ink4a/Arf^{-/-}$ mice to explore how telomere-based crisis relates to the evolution of cancer cell genomes and to tumor biology. The use of *Ink4a/Arf* mutant cells is particularly germane to this study owing to retention of a robust p53-dependent DNA damage response (Kamijo et al. 1998; Frank et al. 2000). With this model system, we sought to determine how progressive telomere attrition correlates with the formation of specific types of chromosomal aberrations and how these cytogenetic abnormalities impact on the biological behavior of these transformed cells in vitro and in vivo.

Results

Severe telomere attrition and dysfunction suppresses the in vitro growth of transformed mouse cells

Early-passage MEF cultures derived from two fifth-generation (G_5) $mTerc^{-/-}$ $Ink4a/Arf^{-/-}$ E13.5 embryos showed a low number of Robertsonian-type p–p arm chromosomal fusions—a *sine qua non* of early telomere dysfunction—by spectral karyotype (SKY) analysis (Blasco et al. 1997; Greenberg et al. 1999; Niida et al. 2000; data not shown). These cultures were cotransfected with *c-MYC* and $H\text{-}RAS^{G12V}$ along with either empty vector (V lines) or *mTerc* (T lines) to produce transformed foci. Multiple foci were subcloned and expanded to generate the independently derived V and T MYC/RAS G_5 $mTerc^{-/-}$ $Ink4a/Arf^{-/-}$ transformed lines used in this study.

For the T lines, reconstitution of telomerase activity and maintenance of telomere length was confirmed at various intervals across >300 passages in cell culture (Fig. 1A; Supplemental Fig. 1A). In contrast, telomerase activity was undetectable in V lines, and mean terminal

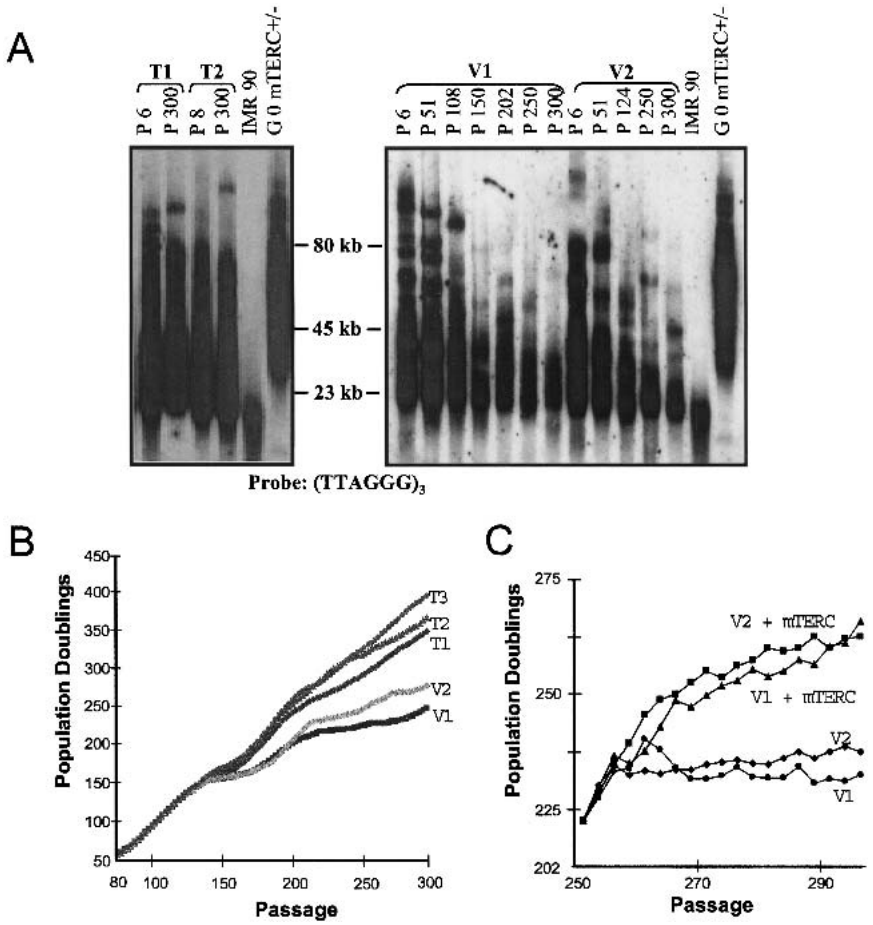

Figure 1. Telomerase activity and telomere dynamics in T and V transformed MEF lines. (*A*) Telomere restriction fragment length analysis of indicated T and V cell lines from passage 6 to 300. Note the gradual decline of telomere length in V cell but not in T cell lines as a function of passage. Human IMR 90 cell line and *mTerc*$^{+/-}$ MEF cell line were included as telomere length standards. Approximate molecular weight standards are shown. (*B*) Growth of T and V cell lines after serial passage via the 3T3 protocol. (*C*) Telomerase reconstitution rescues the growth defects of V cell lines.

restriction fragment (TRF) length of all V lines declined from ~55 to 23 kb over an equivalent passage in cell culture (Fig. 1A; Supplemental Fig. 1A). Correspondingly, telomere PNA-FISH (peptide nucleic acid-*f*luorescence in situ hybridization) analysis of T lines showed retention of robust signal at chromosomal termini over 300 passages, whereas V lines showed a steady passage-dependent increase in signal-free ends (Supplemental Fig. 1B). These baseline studies verify functional reconstitution of telomerase in the T lines and progressive telomere erosion in the V lines over many cell divisions in culture.

Telomere-based crisis has been shown to impair the long-term growth and survival of primary and oncogene-transduced human cells (Counter et al. 1992; Hahn et al. 1999b; Zhang et al. 1999), as well as mouse *mTerc*$^{-/-}$ embryonic stem cells and primary MEFs (Niida et al. 1998; Chin et al. 1999) and murine fibroblasts expressing hTERT (Boklan et al. 2002). To determine the impact of telomere shortening on transformed mouse cells, growth properties of V and T lines were monitored as a function of long-term passage in culture. Over the first ~120 passages, all V and T lines grew at similar rates (Fig. 1B). T line growth rates at later passages were unabated (Fig. 1B). In contrast, commencing at passage 125, the growth rate of V lines slowed and remained retarded through passage 300. We surmise a telomere-based mechanism underlies the V line growth defect, as evidenced by restoration of robust growth after *mTerc* transduction into two independent late passage V cell lines (Fig. 1C). Together, these data support the prevailing view that telomere maintenance enables long-term cellular growth and survival.

Evolving cytogenetic profiles of T and V cell lines on serial passage and tumor formation

We attempted to correlate telomere status and cytogenetic profiles as a function of passage in culture. Examination of three T lines by 4′,6-Diamidino-2-phenylindole (DAPI) staining showed a low number of chromosomal fusions, fragments, and breaks detected from early to late passages, and a complete absence of dicentric chromosomes even at late passages (Fig. 2A,B; data not shown). SKY analysis revealed that the vast majority of fusions were sister chromatid p–p arm fusions involving chromosomes 8 and 12, with only one NRT involving chromosomes 10 and 5 (Fig. 2D; Table 1; Supplemental Fig. 1E).

In sharp contrast, all three V lines showed a steady increase in chromosomal aberrations as a function of passage, corresponding well with the increase in signal-

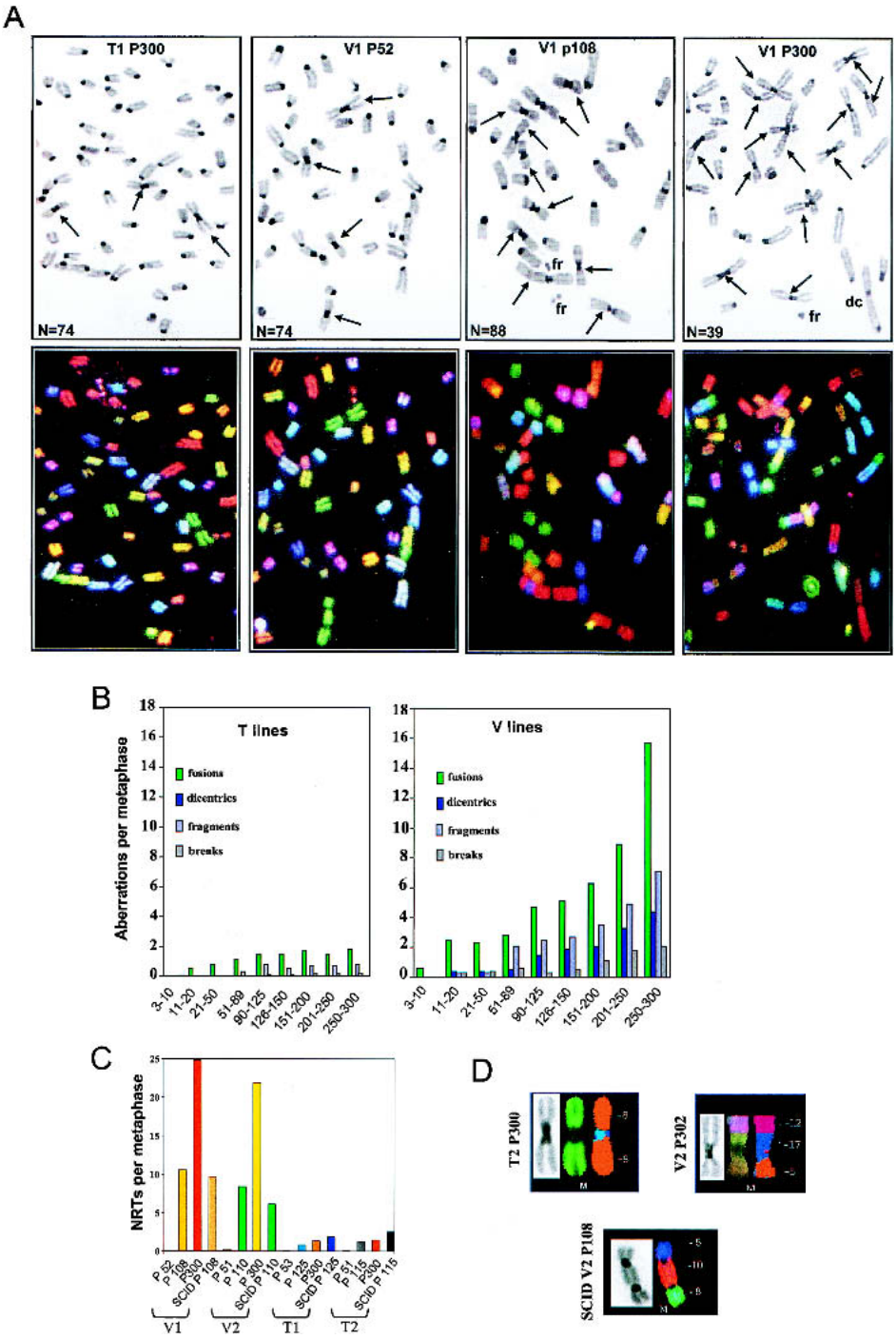

Figure 2. Evolving cytogenetic profiles of T and V cell lines on serial passage. (*A*) Inverse DAPI (*top*) and SKY (*bottom*) analysis of T1 and V1 cell lines at the indicated passages. Note the number of chromosomal translocations in V1 P300 metaphases as revealed by SKY. Arrows indicate p–p arm chromosomal fusions. fr, chromosomal fragments; dc, dicentric chromosome; N, number of chromosomes per metaphase. (*B*) Quantitation of the indicated chromosomal aberrations of three T cell and three V cell lines. (*C*) Quantitation of nonreciprocal translocations (NRTs) found in metaphases prepared from V1, V2, T1, and T2 cell lines, as well as derivative SCID tumors of the indicated passages. (*D*) Representative karyotype of late passage T, V, and derivative SCID tumor cell lines of the indicated passages. Chromosomes are presented as composite inverse DAPI (with dark staining centromeric region), spectral image and, in most cases, computer-classified images. Identities of the translocated chromosome segments are indicated on the *right*.

free ends (Fig. 2B; Supplemental Fig. 1B). Chromosomal fusions represented the most common aberration at late passages (Fig. 2A,B). Telomere repeat signals were not detected at the sites of fusion, in agreement with previ-

Table 1. *Chromosomal aberrations in T and V metaphase spreads analyzed by SKY*

	SKY analysis								
Sample	Lines	Metaphases examined	Average no. chromosomes	Total aberrations per metaphase	Total fusions per metaphase	Rb-like fusions (recurrent) per metaphase	Nonrecurrent NRTs per metaphase	Recurrent NRTs per metaphase	Dicentrics per metaphase
T p18-21	3	30	78.1	0.1	0.4	0.4 T(8;8)	0	0	0
T p95-116	3	25	77.6	1.8	1.8	1.8 T(8;8), (12;12)	0	0	0
T p300	3	26	74.6	4.1	2.9	1.8 T(8;8), (12;12)	1.1 T(10;5)	0	0
SCID T p95-110	2	21	77.2	4.9	4.7	2.3 T(4;4), (8;8), (12;12)	2.4 T(4;12)	0	0
SCID T p300	2	15	76.8	5.3	3.3	2.5 T(8;8), (12;12)	1.8 T(11;12)	0	0
SCID T-2 p300	3	28	76.3	5.6	4.3	2.1 T(8;8), (12;12), (16;16)	2.2 T(11;17); (13;6)	0	0
V p18-20	3	33	61.4	0.9	0.8	0.12 0	0.1	0	0.2
V p98-110	3	45	59.8	14.4	4.8	2.8 T(2;2); (8;8), (13;13)	9.6 T(2;18), (5;2), (13;17), (2;10)	0	1.5 T(11;18;2)
V p300	3	36	36	30.4	15.7	7.2 T(2;2), (5;5), (6;6), (8;8), (13;13), (16;16)	23.2 multiple, complex, involving many chromosomes	0	3.4 T(2;10), (19;2;2)
SCID V p18-21	2	8	63.2	4.1	3.8	T(8;8) (12;12)	1.8	0	0.8
SCID V p98-110	3	24	59.7	15.7	9.3	4.8 T(1;1); (8;8), (10;10), (12;12)	7.9 T(7;9), T(2;10), T(2;13), T(1;7)	2 T(7;11), T(2;13), (3/4 tumors)	2.8 T(5;10;8)
SCID V p300	2	18	37.3	22.5	15.8	5.1 T(1;1), (8;8), (12;12)	16.3 T(12;9;10), T(14;2;12;14) (14;8;8;14)	3 T(12;7), (7;15;8) (7;15;1), (5/5 tumors)	3.1 T(8;7;5)
SCID-2 V p300	4	38	35.5	19.7	16.6	5.3 T(2;2), (8;8), (12;12)	16.7 T(2;17;7), (8;11;11;8)	2 T(12;7;1), (8;7;8)	4.9 T(11;17;3), (8;11;11;8)

Recurrent NRTs are defined as NRTs found in at least three separate metaphases for any given tumor.

ous studies showing that such fusions are a likely by-product of significant telomere erosion (Fig. 4D,E, below; Supplemental Fig. 1B; Blasco et al. 1997; Hande et al. 1999; Hemann et al. 2001). SKY analysis showed that the majority of aberrations in early passage V lines consisted of sister chromatid p–p arm fusions involving chromosomes 8 and 12 (Table 1), similar to those observed in the T lines and consistent with their presence in the parental cultures. In contrast, increased dicentric chromosome formation beginning at passage 90–125 coincided with a striking 116-fold increase in the number of NRTs observed in late passage metaphases (Fig. 2C). By passage 300, a very complex cytogenetic picture was evident, consisting of whole-arm translocations, chromosomal insertions, and other complex structural rearrangements often involving four or five different chromosomes (Fig. 2D; Supplemental Fig. 1E). The vast majority of the observed NRTs were not clonal, raising the possibility that these aberrations were the product of a high rate of ongoing dicentric chromosome formation and BFB cycles and a lack of strong selective pressure to maintain specific chromosomal aberrations in the population.

The nonclonal nature of these chromosomal aberrations in cell culture prompted us to speculate that there exists insufficient biological pressure in vitro to efficiently drive clonal selection of protumorigenic chromosomal aberrations. To address this possibility, T and V lines at passages 18–21, 110, and 300 were used to generate subcutaneous sarcomas in severe combined immunodeficient (SCID) mice for subsequent conventional and SKY cytogenetic analyses. At all passages, T line-derived tumor metaphases were near-tetraploid and contained a low number of nonclonal NRTs per metaphase (Fig. 2C; Table 1). Conversely, in V line-derived sarcomas, increasing passage resulted in a high level of genomic instability in the form of chromosomal fragments and complex structural arrangements, including NRTs involving chromosome 7, which were not detected in any tumors derived from late passage T lines (Supplemental Fig. 1E; Table 1). Analysis of these tumors by array CGH revealed an amplification at the FGF3/4 locus on chromosome 7 (data not shown), consistent with the model in which increased telomere dysfunction results in random double-strand DNA breakage and subsequent amplification of loci governing tumor initiation and progression (O'Hagan et al. 2002; Zhu et al. 2002). It is in-

teresting to note that pretumor genomes possessed an overall higher level of chromosomal instability than did the posttumor genomes, although these NRTs were nonclonal (Fig. 2C). Together, these data are consistent with the view that progressive telomere dysfunction can initiate random levels of regional structural and numerical chromosomal aberrations across a cell population that is then subject to selective forces that drive the clonal expansion of specific aberrations needed for tumorigenic growth.

Telomerase reconstitution endows V lines with metastatic potential

Current human and mouse data are consistent with the hypothesis that telomerase activation plays a role in later stages of tumor progression. To provide experimental support for this hypothesis, we compared both subcutaneous tumor growth and metastatic potential (Stackpole 1981) of early-, mid-, and late-passage T and V lines. In these assays, T lines of all passages (21–23, 125, 306) were robust in their capacity to form subcutaneous tumors and aggressive lung tumor nodules via tail vein injection (0.5–1 mm in size by 1.5 wk after injection; data not shown). By 5 wk after injection, all of these mice were clinically compromised with lesions that replaced 20%–80% of the lung volume and exhibited high-grade malignant histopathological features (Fig. 3A; Table 2). In contrast, passage 18–20 V cell lines seeded the lungs, but the lesions were small (50–150 μm in diameter), numerous (22–63 lesions per mouse), and well-circumscribed—occupying only 5%–20% of lung volume and producing a more benign clinical course (all mice remained healthy at 12 wk after injection; Fig. 3A). All three mid- and late-passage V cell lines showed poor metastatic potential. Although most injected V cell lines seeded the lung parenchyma and were visible as microscopic tumor nodules as early as 1.5 wk after injection (Fig. 3B; Table 2); out of 24 tail-vein injections, only a single well-circumscribed macroscopic lesion measuring 300 μm in diameter emerged 7 wk after injection (Table 2; data not shown). Remarkably, all poorly metastatic V cell lines readily formed subcutaneous tumors after injection into the flanks of SCID mice, although these tumors were consistently smaller than passage-matched T tumors (Supplemental Fig. 2B). Western blot analysis revealed that early-, mid-, and late-passage V lines, as well as their derivative SCID tumor cell lines, continued to express MYC and H-RAS^{G12V} proteins (Supplemental Fig. 2C), indicating that failure to express these oncoproteins was not responsible for the inability of early- and mid-passage V lines to generate lung lesions.

Although multiple independently derived cell lines were used in all assays of this study, loss of metastatic potential could relate to genetic events, other than progressive telomere dysfunction, that accumulated during prolonged passage in culture. We therefore assessed the impact of *mTerc* reconstitution on passage 18–20, 98–110, and 305–310 V cell lines. Transduction of *mTerc*, but not an empty vector, restored telomerase activity (Supplemental Fig. 2A), reduced the number of signal-free ends (data not shown), and conferred enhanced growth potential in low-density seeding assays to V cell lines at all three passages (Supplemental Fig. 1C,D; data not shown). In the metastasis assay, three of three independently derived *mTerc*-reconstituted early passage; three of three mid-passage and two of two late-passage V cell lines injected into a total of 41 mice seeded the lungs at very high efficiencies, obliterating 25%–90% of the normal lung parenchyma as early as 1.5 wk after injection (Fig. 3B; data not shown). These aggressive *mTerc*-reconstituted tumors resulted in death by 3 wk. In contrast, mice injected with empty vector-reconstituted early-, mid-, and late-passage V cell lines remained free of macroscopic metastatic lung lesions 12 wk after injection, although on examination of multiple serial paraffin sections, two or three microscopic tumor nodules were often detected within the lung parenchyma (Fig. 3B; data not shown). These results indicate that although V cell lines were able to seed the lungs in the tail-vein metastasis assay, they were unable to proliferate after seeding. Together, these data strongly support the hypothesis that telomerase plays an important role in facilitating advanced stages of tumor development and growth.

Telomerase-independent telomere lengthening in V line-derived tumors and its lack of biological equivalence to telomerase

The capacity of late-passage V cell lines to form subcutaneous sarcomas suggested either sufficient telomere reserve for tumorigenesis or activation of ALT. To monitor the capacity for ALT activation, these sarcomas were used to generate additional serial tumors in SCID mice. After a second round of subcutaneous SCID tumor formation, resulting sarcomas were extremely aggressive and grew to 2 cm in size as early as 1 wk after injection (Table 2). These sarcoma cell lines (referred to as SCID-2 V or T cell lines) displayed rapid growth in culture, with a population doubling time of ~12 h compared with a population doubling of ~29 h in the parental lines (data not shown). The wild-type status of p53 in these tumor cell lines was confirmed by the rapid induction of p53 and p21 levels after γ irradiation (data not shown). TRF Southern analysis showed dramatic telomere lengthening and heterogeneity (ranging in length from 15 to >100 kb) in five independently derived SCID-2 V cell tumor lines compared with the parental cell lines, a pattern characteristic of human ALT cell lines (Fig. 4A; Lansdorp et al. 1997; Yeager et al. 1999; data not shown). Tumors derived from three telomerase-positive SCID-2 T cell lines do not show this TRF length heterogeneity (Fig. 4A; data not shown). Correspondingly, PNA-FISH revealed a wide range of telomere signal intensity in every metaphase of all five SCID-2 tumor V cell lines (Fig. 4B; data not shown). Of note, a significant number of signal free ends were still detected, although there were many termini with robust telomeric signal (Fig. 4, cf. B and D). These features are consistent with telomere length het-

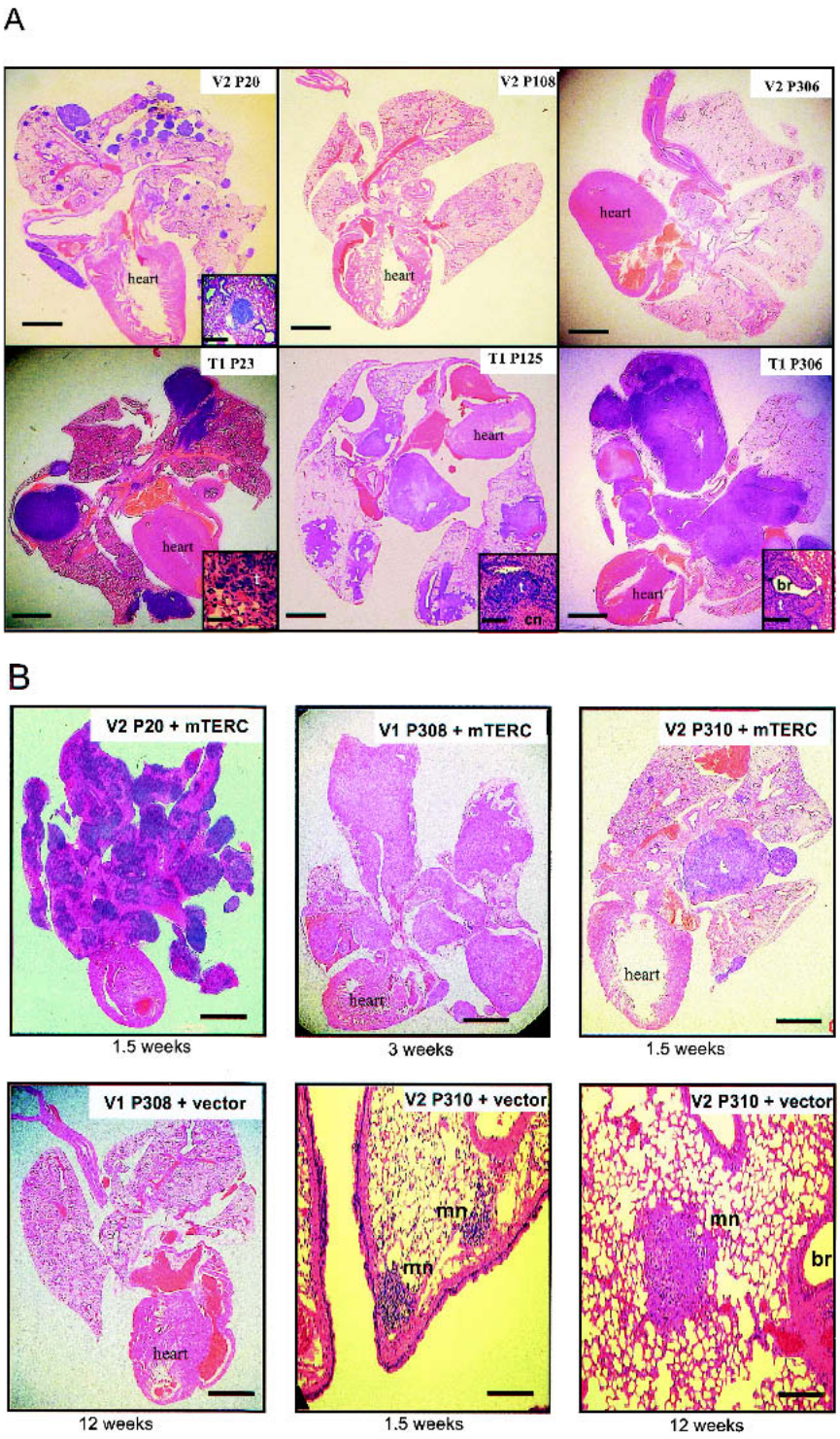

Figure 3. Telomerase expression confers metastatic potential. (*A*) 5×10^5 tumor cells from early-, mid-, and late-passage V and T cell lines were injected into the tail vein of SCID mice. Mice were killed after 4 wk, and their lungs were examined for tumor seeding, both grossly and by 10-µm serial sections with H&E staining. All photographs were taken at 5× magnification unless otherwise indicated. Injection of early passage V2 tumor cells resulted in multiple tumor nodules scattered throughout the lung parenchyma. Inset are 40× magnification views of a tumor nodule within the lung. Injection of mid- and late-passage V2 cells did not result in tumor seeding within the lungs. Injection of T1 tumor cells at all passages resulted in tumors obliterating ~40% to 80% of lungs. Insets show 40× magnification views of the tumor cells. The tumors were poorly differentiated, with large pleomorphic nuclei and multiple nucleoli. Tumors (t) often surrounded and compressed bronchioles (br) and contained regions of central necrosis (cn). Bars, 15 mm for gross photos, 100 µm for insets. (*B*) Tail-vein injections of *mTerc*-reconstituted late-passage V cell lines resulted in massive tumors that obliterated >90% of normal lung tissue. Tumor nodules were apparent as early as 1.5 wk after injection. P20 V cell line reconstituted with telomerase activity and injected intravenously into SCID mice yielded numerous lung tumors after 3 wk. Late-passage V lines reconstituted with vector-alone control did not form tumors 12 wk after injection, although microscopic lesions were observed within the lungs of most injected mice as early as 1.5 wk after injection. Bars, 15 mm for whole mounts, 50 µ for 20× photomicrographs.

erogeneity and were not observed in parental passage 300 V cell lines (Fig. 4D) or in any of the SCID-2 T cell lines (data not shown).

All human ALT cell lines, but no telomerase-positive cell lines, are characterized by the presence of ALT-associated promyelocytic leukemia bodies (APBs) containing the PML protein, low-molecular-weight telomeric DNA, and telomere associated proteins, including TRF1 (Yeager et al. 1999; Perrem et al. 2001). Immunofluorescence analysis revealed that in a subpopulation (~10%) of interphase cells, TRF1 colocalized with PML in brightly staining nuclear structures resembling APBs in all five SCID-2 tumor V cell lines exhibiting telomere length heterogeneity (Fig. 4F; data not shown). These structures were not observed in passage 300 parental V cell lines or in the SCID-2 T cell lines (Fig. 4G; data not shown),

Table 2. *Summary of SCID mice T and V tumor cell line injection experiments*

	Metastatic assay					Sc. injections
Cell lines	No. of lines injected	No. mice injected	Macroscopic tumors >20% lungs	Microscopic tumors 50–250 μ dia.	Time of death after injection	Time to form tumors to 2 cm size
V p18-20	2	8	5/8	2/8	>12 wk	5–6 wk
V p98-110	3	12	1/12*	5/12	>12 wk	5–6 wk
V p300	3	12	0/12	7/12	>12 wk	5–7 wk
V p18-20 + mTERC	3	12	8/12	n.a.	1.5–3 wk	4–6 wk
V p98-110 + mTERC	3	21	17/21	2/21	1.5–3 wk	4–6 wk
V p305-310 + mTERC	2	8	8/12	1/12	1.5–3 wk	4–6 wk
V p18-21 + vector	2	4	0/4	3/4	>12 wk	5–7 wk
V p98-110 + vector	3	8	0/8	3/8	>12 wk	5–7 wk
V p305-310 + vector	3	9	0/9	2/9	>12 wk	6–8 wk
SCID V p6	1	4	0/4	2/4	>12 wk	6–12 wk
SCID V p108-110	2	9	0/9	5/9	>12 wk	7–11 wk
SCID-1 V p300	2	12	0/12	6/12	>12 wk	4–8 wk
SCID-2 V p300	5	15	0/15	8/15	sac at 7 wk	1–2 wk
SCID-2V p300 + mTERC	5	15	15/15	n.a.	5 wk	n.d.
T p21-25	3	7	6/7	0/7	5–6 wk	4.5 wk
T p125	1	4	4/4	n.a.	4–5 wk	4–4.5 wk
T p300	3	12	10/12	2/12	4–5 wk	4–5 wk
SCID T p23	1	6	6/6	n.a.	4–5 wk	4–5 wk
SCID T p125	1	7	2/7	2/7	5–6 wk	5–6 wk
SCID-1 T p300	2	8	6/8	1/8	4–5 wk	4–5 wk
SCID-2 T p300	3	12	8/12	2/12	4–5 wk	4–5 wk
G0 mTERC+/–	2	4	4/4	n.a.	3–4 wk	4–6 wk
G2 mTERC–/–	2	4	4/4	n.a.	3–4 wk	4–6 wk

*This lesion was 300 μ in diameter.
n.d. indicates not done; n.a. indicates not applicable (macroscopic tumors obliterated lung field).

consistent with previous analyses of ALT human cells (Lansdorp et al. 1996). Enrichment of the G_2 phase of the cell cycle by double thymidine block followed by Hoechst 33342 treatment led to a threefold increase in the number of APBs observed in three of three SCID-2 V cell lines examined (Fig. 4H), consistent with the observation that APBs are predominantly found in the G_2 phase (Grobelny et al., 2000; Wu et al., 2000). Taken together, these data indicate that extensively passaged V cell lines can activate ALT under the biological pressure of tumorigenesis in vivo, and that the ALT pathway enhances in vitro growth and subcutaneous tumor potential.

The consistent presence of telomere maintenance mechanism in advanced human cancers has supported the assumption that the major factor in the promotion of full malignant transformation is adequate telomere reserves, and that the particular telomere maintenance mechanism used was less relevant. We therefore tested ALT+ cell lines for metastatic activity and established that despite robust subcutaneous tumor growth, five of five independently derived ALT+ SCID-2 V lines failed to yield macroscopic lung tumors up to 7 wk after tail-vein injection, although small microscopic metastatic nodules were detected in lungs as early as 1.5 wk after injection (Fig. 4I; Table 2). In contrast, all 5 ALT+ cell lines reconstituted with telomerase activity formed macroscopic tumor nodules 1.5 wk after injection, and these lesions evolved into massive tumors that completely filled the lung parenchyma and led to the demise of injected animals by 5 wk (Fig. 4I). We conclude that ALT-mediated telomere maintenance is not functionally equivalent to telomerase-mediated telomere maintenance in facilitating tumor progression, particularly metastasis.

Discussion

In this study, we show that extended in vitro passage of transformed *mTerc*$^{-/-}$ *Ink4a/Arf*$^{-/-}$ mouse cell lines culminates in a state of severe telomere shortening, cytogenetic aberrations, and growth defects remarkably similar to crisis (or M_2) in human cells (Counter et al. 1992). By conducting an exhaustive serial analysis of these cultures, it was possible to establish a very tight correlation between the appearance of unstable dicentric chromosomes (as opposed to p–p arm Robertsonian fusions), the emergence of NRTs, a proliferative growth defect in vitro, and loss of metastatic potential in vivo. The defect in transformed cellular growth in the setting of progressive telomere dysfunction is similar to previous observations on extensive passage of untransformed late generation *mTerc*$^{-/-}$ cultures (Greenberg et al. 1999; Niida et al. 2000; Espejel and Blasco 2002). Our studies extend these observations by establishing a temporal correlation between the formation of dicentrics and nonreciprocal translocations and the altered biological properties of these transformed cells.

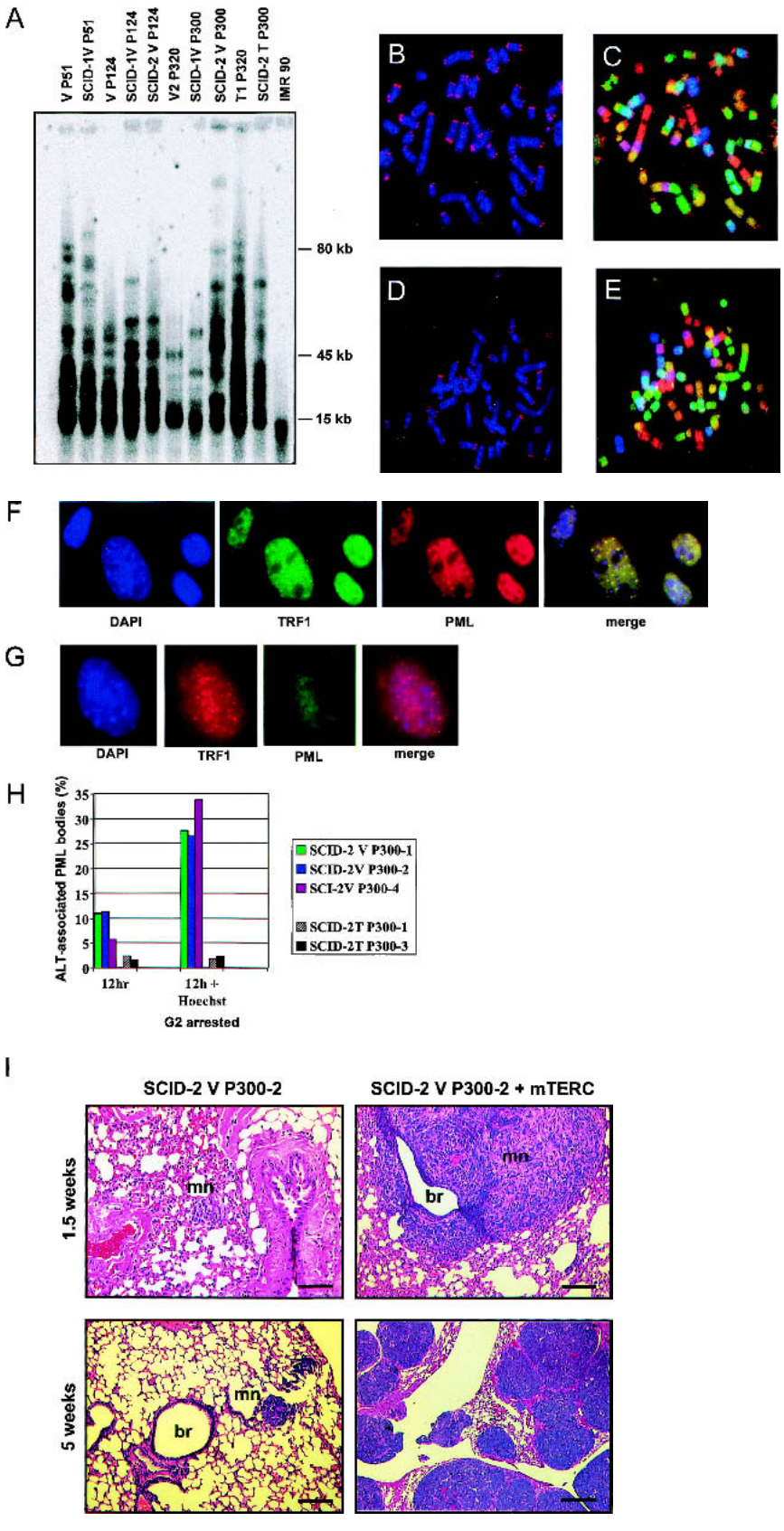

Figure 4. Telomerase-independent telomere lengthening in SCID V tumors. (*A*) TRF Southern analysis of SCID tumors derived from p300 V cell lines show progressive telomere lengthening. Passage 300 V cell lines injected into SCID mice yielded SCID-1 V P300 sarcomas. Cell lines generated from this tumor were reinjected into SCID mice to generate SCID-2 V P300 sarcomas. Note the heterogenous telomere length of SCID-2 V P300 cells. (*B*) PNA-FISH analysis of metaphase generated from SCID-2 V P300 tumor. Note the number of chromosomal ends possessing long telomeres. (*C*) SKY was performed on the same metaphases shown in *B*. Telomere signals do not localize to sites of chromosomal fusion. (*D*) PNA-FISH analysis of a passage 300 parental V cell line. (*E*) SKY analysis of the same metaphase shown in *D*. (*F*) Immunofluorescence analysis of ALT-positive cells. SCID-2 V p300 cell lines were stained with the indicated antibodies to reveal colocalization of TRF1 and PML in ALT foci. (*G*) ALT foci were not detected within nuclei of parental passage 300 V cell lines. Note that TRF1 stains in a speckled pattern characteristic of telomere localization. (*H*) ALT foci are enriched approximately threefold in the G_2 phase of the cell cycle after double-thymidine block and treatment of SCID-2 ALT V cell lines with Hoechst 33342, which specifically arrests cells in G_2. Non-ALT SCID-2 T cell lines do not enrich for ALT foci after synchronization and Hoechst treatment. (*I*) SCID-2 ALT V cell lines seed the lungs as microscopic metastatic nodules (mn) as early as 1.5 wk after injection but do not grow substantially larger. In contrast, SCID-2 ALT V cell lines reconstituted with telomerase efficiently formed macroscopic metastatic lesions that obliterated normal lung parenchyma after 5 wk. br, bronchiole. Bars: 50μ for 20× photomicrographs, 1.5 mm for 2.5× photomicrograph.

Previous work has shown that severe telomere dysfunction can engender a level of chromosomal instability that can promote tumorigenesis, particularly in circumstances of p53 deficiency. The data of this study show that telomere maintenance, specifically by telomerase reactivation, is required for these "initiated" cancer cells to achieve their full malignant potential, including metastasis. The molecular changes necessary for the acquisition of an invasive and metastatic phenotype are highly complex and involve a series of diverse cellular processes that must be completed in order to establish secondary tumor foci at distant organs (for review, see Hanahan and Weinberg 2000). One such process appears to be telomerase expression, because human tumor cells with metastatic potential often express high levels of telomerase (Chadeneau et al. 1995; Saito et al. 1997; Tang et al. 1998; Balcom et al. 2001), a pattern of expression consistent with its role during tumor progression (Counter et al. 1994). Although all V lines possessed subcutaneous tumorigenic potential and were able to transit through the bloodstream, seed the lungs, and form microscopic tumors in an in vivo metastatic assay, mid- and late-passage V lines with moderate to severe telomere dysfunction were incapable of generating macroscopic lesions within the lung parenchyma. Functional reconstitution of telomerase activity via ectopic expression of *mTerc* rendered these V lines competent to form large metastatic lesions, which ultimately compromised the host animal. The observation that all *mTerc*-reconstituted V cell lines formed aggressive metastatic lesions in the lungs as early as 1.5 wk after intravenous injection favors the view that repair of dysfunctional telomeres, and not the de novo acquisition of rare mutations, enabled metastatic tumor progression. Our data further suggest that even if cancer cells have acquired all of the changes necessary for tumorigenesis, ongoing checkpoint responses elicited by telomere dysfunction alone can limit the metastatic potential of prometastatic genetic lesions present in the population. It is possible that reconstituted telomerase stabilizes the genome from further BFB cycles and quells the DNA damage checkpoint response to a level permissive for unencumbered tumor growth within the lung parenchyma. Along these lines, it is interesting to note there was increased steady state basal expression of p53 in the V lines compared to equivalently passaged T lines (data not shown).

We show that late-passage V cell lines readily formed subcutaneous tumors when injected subcutaneously into SCID mice. Multiple rounds of in vivo tumor formation activated the ALT pathway to lengthen telomeres and enhance tumor growth. The activation of ALT in this setting could relate to the strong selection pressures of cells in crisis to maintain telomere lengths during tumor formation. ALT has been shown previously to maintain telomeres of *mTerc*-null cell lines during long-term passages in vitro (Hande et al. 1999; Niida et al. 2000). However, in contrast to mTerc-reconstituted ALT+ cell lines, nontransduced controls were unable to generate macroscopic metastatic lesions in the lungs, suggesting that telomere maintenance via ALT cannot functionally substitute for telomerase. One possible explanation is that the telomere length heterogeneity characteristic of ALT cells renders a population of chromosome ends with very long telomeres, whereas other termini have denuded dysfunctional telomeres (Lansdorp et al. 1996; Perrem et al. 2001). A single marked telomere in ALT cells exhibited gradual shortening over time in culture, followed by rapid increases in length and resumption of telomere attrition (Murnane et al. 1994). This cyclical nature of telomere dynamics in ALT cells suggests that a biologically relevant steady-state level of dysfunctional telomeres might exist in these cells, possibly limiting cellular growth during metastasis, perhaps by activation of p53. In contrast, recent evidence suggest that restoration of telomerase activity preferentially repaired the shortest telomeres and rescued cellular defects owing to telomere dysfunction (Hemann et al. 2001; Samper et al. 2001). Although the molecular mechanisms involved in mammalian ALT still remain unclear, current evidence suggests that telomere-telomere recombination is involved (Dunham et al. 2000). Our SCID-2 ALT V cell lines now provide an opportunity to further dissect the molecular mechanisms driving ALT in mammalian cells in an in vivo setting.

In addition, recent evidence suggests that telomerase has additional roles beyond those involved in telomere maintenance (Stewart et al. 2002; for review, see Chang and DePinho 2002). In transgenic mice, overexpression of telomerase in basal keratinocytes resulted in increased incidence of carcinogen-induced skin tumors (Gonzalez-Suarez et al. 2001), whereas overexpression of telomerase in mammary glands promoted the development of spontaneous cancers (Artandi et al. 2002). Furthermore, ectopic expression of hTERT in human mammary cells that have epigenetically silenced p16 resulted in increased resistance to growth arrest mediated by transforming growth factor-β (Stampfer et al. 2001). Taken together, these results raise the possibility of a telomere-independent role for telomerase in signaling cellular proliferation. It is formally possible that, in addition to repairing dysfunctional telomeres, ectopic expression of telomerase in late-passage V cell lines confers a certain growth advantage needed for metastatic activity.

Our findings may have implications for the use of telomerase inhibitors as antitumor agents in human cancers. Inhibition of telomerase will put tumors that are initially telomerase positive under strong selection pressure to activate ALT. Because repression of ALT results in senescence and cell death (Nakabayashi et al. 1997; Perrem et al. 1999), ALT, like telomerase, may be an attractive drug target. The use of both classes of drugs to inhibit telomere maintenance in tumor cells may help prevent the emergence of drug resistance. In addition, despite concerns for activation of ALT in the course of telomerase treatment, these studies suggest that ALT cells may not be as biologically robust as telomerase-positive cancer cells and may succumb to drug intervention despite activation of the ALT pathway.

Materials and methods

Cell culture, transformation assay, 3T3 assay, and cell-cycle synchronization

MEFs were prepared from individual day 13.5 embryos derived from second- and fifth-generations *mTerc*$^{-/-}$ *Ink4a/Arf*$^{-/-}$ mice. Two independently derived parental cultures were cotransfected with MYC and H-RAS^{G12V}, and either *mTerc* (T) or empty vector (V), to generate transformed foci as previously described (Blasco et al. 1997; Greenberg et al. 1999). Individual foci were isolated and expanded into 10-cm plates that were designated as passage 1 (P1) lines. A total of three T lines and three V lines were generated from each parental culture. Serial passages of cell lines were performed according to the NIH3T3 protocol (Todaro and Green 1963). The population-doubling number (PD) of each passage was calculated as described (Blasco et al. 1997). Low-density seeding assays were performed as described (Greenberg et al. 1999). For reconstitution of telomerase activity, 5 μg of *mTerc* vector and 0.5 μg of pBABE-puro vector were cotransfected into indicated V and T cell lines; 2 μg/mL of puromycin was used to select for stable clones. To enrich for cells at G_2, cells were plated onto coverslips, synchronized by double-thymidine block as described (Detke et al. 1979), followed by addition of Hoeschst 33342 at a final concentration of 0.5 μg/mL for 12 h more. Cells were washed and processed for immunofluorescence as described below.

Pulse-field gel electrophoresis

MEFs (2.5×10^4) were imbedded into 0.8% agarose plugs and then digested overnight with 200 U of restriction enzymes *Hin*fI and *Rsa*I. DNA was resolved with a 0.8% agarose gel with a CHEF pulse-field apparatus according to manufacturer's suggestions (Bio-Rad). The gel was dried, denatured, hybridized to 5′-[γ^{32}P]T_2AG_3 telomeric DNA oligonucleotides, and autoradiographed, as described (Blasco et al. 1997).

Telomerase assays, telomere FISH, and SKY analysis

TRAP assays were performed with the TrAPeze kit (Oncor) as described (Greenberg et al. 1998). Metaphase chromosomes from transformed MEFs of various passages were prepared as described (Rudolph et al. 1999), and FISH of telomeric sequences with Cy-3-labeled T_2AG_3 PNA probe were performed as described (Greenberg et al. 1999). SKY was performed as described (Artandi et al. 2000) according to manufacturer's recommendations by using mouse chromosome paint probes (Applied Spectral Imaging) on a Nikon Eclipse 800 microscope equipped with an ASI interferometer and workstation. Depending on the quality of metaphase spreads, 8–15 metaphases from each sample were analyzed in detail.

Immunofluorescence and Western analyses

Cells were grown on coverslips, permeablized in 0.5% NP-40 in PBS, fixed with 4% paraformaldehyde, and blocked with 0.2% gelatin and 0.5% BSA. For immunofluorescence, rabbit anti-mouse TRF1 antipeptide antibody #644 (a kind gift from Dr. Titia de Lange, Rockefeller University, New York) was diluted 1:2000, goat anti-TRF1 E-15 and rabbit anti-PML H-238 and PML mAB PG-M3 (Santa Cruz) antibodies were diluted 1:100 and incubated overnight, followed by Rh- or FITC-labeled secondary antibody (Vector Laboratories). DAPI was used to stain cell nuclei. For Western analysis, cells were trypsinized and lysed in RIPA buffer, and 30 μg of lysate per late was resolved by SDS-PAGE and transferred onto PVDF membranes for c-MYC and H-RAS immunoblots. The antibodies used for Western analyses were antimouse c-Myc (9E10; 1:500, Santa Cruz), antirabbit H-Ras (C20; 1:500; Santa Cruz), and antigoat actin (I-19; 1:2000; Santa Cruz) for loading control. Western blots assays were performed in accordance with standard procedures by using ECL detection (Amersham).

SCID injections and metastatic seeding assay

T and V cell lines (1×10^6 cells/mL) at different passages were injected into both flanks of SCID mice (0.5 mL/site of injection). Four mice were injected per tumor cell line. Tumor size was measured three times a week, and mice were killed when tumors reached 2 cm in diameter. Tumors were harvested and split into three equal parts: one for hematoxylin and eoisin (H&E) analysis, one for genomic DNA isolation, and one adapted to cell culture (RPMI, 10% FCS, 1× Pen/Strep). Tumor cells were processed to generate metaphase spreads for PNA-FISH and SKY analysis. For the metastatic seeding assays, T and V cell lines were resuspended in Hanks buffer at 1×10^6 cells/mL, and 0.5 mL was injected into the tail vein of SCID mice. Mice were killed at 1–12 wk after injection or when they appeared ill. Autopsies performed to look for tumor seeding at distant organs, and gross tumor sizes were measured before organs were harvested for H&E analysis.

Acknowledgments

We wish to thank Jiang Shan for SCID tail-vein injections, Christine Lam for processing histopathology samples, Titia de Lange for TRF1 antibody, and Norman Sharpless for insightful comments. S.C. is supported by a KO8 Mentored Award (1KO8AG01019-01) from the NIA, an Ellison New Scholar in Aging Award from the Ellison Medical Foundation, and the Dana Farber Cancer Institute Claudia Adams Barr Program in Cancer Research. R.S.M. is supported by a Damon Runyon Cancer Research Fellowship DRG-1701-02. R.A.D. is an American Cancer Society Professor and a Steven and Michele Kirsch Investigator.

The publication costs of this article were defrayed in part by payment of page charges. This article must therefore be hereby marked "advertisement" in accordance with 18 USC section 1734 solely to indicate this fact.

References

Allsopp, R.C., Vaziri, H., Patterson, C., Goldstein, S., Younglai, E.V., Futcher, A.B., Greider, C.W., and Harley, C.B. 1992. Telomere length predicts replicative capacity of human fibroblasts. *Proc. Natl. Acad. Sci.* **89:** 10114–10118.

Artandi, S.E., Chang, S., Lee, S.L., Alson, S., Gottlieb, G.J., Chin, L., and DePinho, R.A. 2000. Telomere dysfunction promotes non-reciprocal translocations and epithelial cancers in mice. *Nature* **406:** 641–645.

Artandi, S.E., Alson, S., Tietze, M.K., Sharpless, N.E., Ye, S., Greenberg, R.A., Castrillon, D.H., Horner, J.W., Weiler, S.R., Carrasco, R.D., et al. 2002. Constitutive telomerase expression promotes mammary carcinomas in aging mice. *Proc. Natl. Acad. Sci.* **99:** 8191–8196.

Balcom, J.H.t., Keck, T., Warshaw, A.L., Antoniu, B., Graeme-Cook, F., and Fernandez-del Castillo, C. 2001. Telomerase activity in periampullary tumors correlates with aggressive malignancy. *Ann. Surg.* **234:** 344–350; discussion 350–351.

Blackburn, E.H. 2001. Switching and signaling at the telomere.

Cell **106:** 661–673.

Blasco, M.A., Lee, H.W., Hande, M.P., Samper, E., Lansdorp, P.M., DePinho, R.A., and Greider, C.W. 1997. Telomere shortening and tumor formation by mouse cells lacking telomerase RNA. *Cell* **91:** 25–34.

Bodnar, A.G., Ouellette, M., Frolkis, M., Holt, S.E., Chiu, C.P., Morin, G.B., Harley, C.B., Shay, J.W., Lichtsteiner, S., and Wright, W.E. 1998. Extension of life-span by introduction of telomerase into normal human cells. *Science* **279:** 349–352.

Bohr, V.A. and Dianov, G.L. 1999. Oxidative DNA damage processing in nuclear and mitochondrial DNA. *Biochimie* **81:** 155–160.

Boklan, J., Nanjangud, G., MacKenzie, K.L., May, C., Sadelain, M., and Moore, M.A. 2002. Limited proliferation and telomere dysfunction following telomerase inhibition in immortal murine fibroblasts. *Cancer Res.* **62:** 2104–2114.

Bryan, T.M., Englezou, A., Dalla-Pozza, L., Dunham, M.A., and Reddel, R.R. 1997. Evidence for an alternative mechanism for maintaining telomere length in human tumors and tumor-derived cell lines. *Nat. Med.* **3:** 1271–1274.

Chadeneau, C., Hay, K., Hirte, H.W., Gallinger, S., and Bacchetti, S. 1995. Telomerase activity associated with acquisition of malignancy in human colorectal cancer. *Cancer Res.* **55:** 2533–2536.

Chang, S. and DePinho, R.A. 2002. Telomerase extracurricular activities. *Proc. Natl. Acad. Sci.* **99:** 12520–12522.

Chin, L., Artandi, S.E., Shen, Q., Tam, A., Lee, S.L., Gottlieb, G.J., Greider, C.W., and DePinho, R.A. 1999. p53 deficiency rescues the adverse effects of telomere loss and cooperates with telomere dysfunction to accelerate carcinogenesis. *Cell* **97:** 527–538.

Counter, C.M., Avilion, A.A., LeFeuvre, C.E., Stewart, N.G., Greider, C.W., Harley, C.B., and Bacchetti, S. 1992. Telomere shortening associated with chromosome instability is arrested in immortal cells which express telomerase activity. *EMBO J.* **11:** 1921–1929.

Counter, C.M., Hirte, H.W., Bacchetti, S., and Harley, C.B. 1994. Telomerase activity in human ovarian carcinoma. *Proc. Natl. Acad. Sci.* **91:** 2900–2904.

de Lange, T. 1995. Telomere dynamics and genomic instability in human cancer. In *Telomeres* (eds. E.H. Blackburn and C.W. Greider), pp. 265–293. Cold Spring Harbor Laboratory Press, Cold Spring Harbor, NY.

de Lange, T., Shiue, L., Myers, R.M., Cox, D.R., Naylor, S.L., Killery, A.M., and Varmus, H.E. 1990. Structure and variability of human chromosome ends. *Mol. Cell. Biol.* **10:** 518–527.

Detke, S., Lichtler, A., Phillips, I., Stein, J., and Stein, G. 1979. Reassessment of histone gene expression during cell cycle in human cells by using homologous H4 histone cDNA. *Proc. Natl. Acad. Sci.* **76:** 4995–4999.

Dunham, M.A., Neumann, A.A., Fasching, C.L., and Reddel, R.R. 2000. Telomere maintenance by recombination in human cells. *Nat. Genet.* **26:** 447–450.

Elledge, S.J. 1996. Cell cycle checkpoints: Preventing an identity crisis. *Science* **274:** 1664–1672.

Espejel, S. and Blasco, M.A. 2002. Identification of telomere-dependent "senescence-like" arrest in mouse embryonic fibroblasts. *Exp. Cell Res.* **276:** 242–248.

Frank, K.M., Sharpless, N.E., Gao, Y., Sekiguchi, J.M., Ferguson, D.O., Zhu, C., Manis, J.P., Horner, J., DePinho, R.A., and Alt, F.W. 2000. DNA ligase IV deficiency in mice leads to defective neurogenesis and embryonic lethality via the p53 pathway. *Mol. Cell* **5:** 993–1002.

Gisselsson, D., Pettersson, L., Hoglund, M., Heidenblad, M., Gorunova, L., Wiegant, J., Mertens, F., Dal Cin, P., Mitelman, F., and Mandahl, N. 2000. Chromosomal breakage-fusion-bridge events cause genetic intratumor heterogeneity. *Proc. Natl. Acad. Sci.* **97:** 5357–5362.

Gonzalez-Suarez, E., Samper, E., Flores, J.M., and Blasco, M.A. 2000. Telomerase-deficient mice with short telomeres are resistant to skin tumorigenesis. *Nat. Genet.* **26:** 114–117.

Gonzalez-Suarez, E., Samper, E., Ramirez, A., Flores, J.M., Martin-Caballero, J., Jorcano, J.L., and Blasco, M.A. 2001. Increased epidermal tumors and increased skin wound healing in transgenic mice overexpressing the catalytic subunit of telomerase, mTERT, in basal keratinocytes. *EMBO J.* **20:** 2619–2630.

Greenberg, R.A., Allsopp, R.C., Chin, L., Morin, G.B., and DePinho, R.A. 1998. Expression of mouse telomerase reverse transcriptase during development, differentiation and proliferation. *Oncogene* **16:** 1723–1730.

Greenberg, R.A., Chin, L., Femino, A., Lee, K.H., Gottlieb, G.J., Singer, R.H., Greider, C.W., and DePinho, R.A. 1999. Short dysfunctional telomeres impair tumorigenesis in the INK4a(δ2/3) cancer-prone mouse. *Cell* **97:** 515–525.

Greider, C.W. 1996. Telomere length regulation. *Annu. Rev. Biochem.* **65:** 337–365.

Grobelny, J.V., Godwin, A.K., and Broccoli, D. 2000. ALT-associated PML bodies are present in viable cells and are enriched in cells in the G^2/M phase of the cell cycle. *J. Cell Sci.* **113 (Pt 24):** 4577–4585.

Hahn, W.C., Counter, C.M., Lundberg, A.S., Beijersbergen, R.L., Brooks, M.W, and Weinberg, R.A. 1999a. Creation of human tumour cells with defined genetic elements. *Nature* **400:** 464–468.

Hahn, W.C., Stewart, S.A., Brooks, M.W, York, S.G., Eaton, E., Kurachi, A., Beijersbergen, R.L., Knoll, J.H., Meyerson, M., and Weinberg, R.A. 1999b. Inhibition of telomerase limits the growth of human cancer cells. *Nat. Med.* **5:** 1164–1170.

Hanahan, D. and Weinberg, R.A. 2000. The hallmarks of cancer. *Cell* **100:** 57–70.

Hande, M.P., Samper, E., Lansdorp, P., and Blasco, M.A. 1999. Telomere length dynamics and chromosomal instability in cells derived from telomerase null mice. *J. Cell Biol.* **144:** 589–601.

Hara, E., Tsurui, H., Shinozaki, A., Nakada, S., and Oda, K. 1991. Cooperative effect of antisense-Rb and antisense-p53 oligomers on the extension of life span in human diploid fibroblasts, TIG-1. *Biochem. Biophys. Res. Commun.* **179:** 528–534.

Harley, C.B., Futcher, A.B., and Greider, C.W. 1990. Telomeres shorten during ageing of human fibroblasts. *Nature* **345:** 458–460.

Hastie, N.D., Dempster, M., Dunlop, M.G., Thompson, A.M., Green, D.K., and Allshire, R.C. 1990. Telomere reduction in human colorectal carcinoma and with ageing. *Nature* **346:** 866–868.

Hemann, M.T., Strong, M.A., Hao, L.Y., and Greider, C.W. 2001. The shortest telomere, not average telomere length, is critical for cell viability and chromosome stability. *Cell* **107:** 67–77.

Kamijo, T., Weber, J.D., Zambetti, G., Zindy, F., Roussel, M.F., and Sherr, C.J. 1998. Functional and physical interactions of the ARF tumor suppressor with p53 and Mdm2. *Proc. Natl. Acad. Sci.* **95:** 8292–8297.

Kim, N.W., Piatyszek, M.A., Prowse, K.R., Harley, C.B., West, M.D., Ho, P.L., Coviello, G.M., Wright, W.E., Weinrich, S.L., and Shay, J.W. 1994. Specific association of human telomerase activity with immortal cells and cancer. *Science* **266:** 2011–2015.

Lansdorp, P.M., Verwoerd, N.P., van de Rijke, F.M., Dragowska,

V., Little, M.T., Dirks, R.W., Raap, A.K., and Tanke, H.J. 1996. Heterogeneity in telomere length of human chromosomes. *Hum. Mol. Genet.* **5:** 685–691.

Lansdorp, P.M., Poon, S., Chavez, E., Dragowska, V., Zijlmans, M., Bryan, T., Reddel, R., Egholm, M., Bacchetti, S., and Martens, U. 1997. Telomeres in the haemopoietic system. *Ciba Found. Symp.* **211:** 209–218.

Lengauer, C., Kinzler, K.W., and Vogelstein, B. 1998. Genetic instabilities in human cancers. *Nature* **396:** 643–649.

Maser, R.S. and DePinho, R.A. 2002. Connecting chromosomes, crisis, and cancer. *Science* **297:** 565–569.

McClintock, B. 1941. The stability of broken ends of chromosomes in Zea mays. *Genetics* **26:** 234–282.

Murnane, J.P., Sabatier, L., Marder, B.A., and Morgan, W.F. 1994. Telomere dynamics in an immortal human cell line. *EMBO J.* **13:** 4953–4962.

Nakabayashi, K., Ogata, T., Fujii, M., Tahara, H., Ide, T., Wadhwa, R., Kaul, S.C., Mitsui, Y., and Ayusawa, D. 1997. Decrease in amplified telomeric sequences and induction of senescence markers by introduction of human chromosome 7 or its segments in SUSM-1. *Exp. Cell Res.* **235:** 345–353.

Niida, H., Matsumoto, T., Satoh, H., Shiwa, M., Tokutake, Y., Furuichi, Y., and Shinkai, Y. 1998. Severe growth defect in mouse cells lacking the telomerase RNA component. *Nat. Genet.* **19:** 203–206.

Niida, H., Shinkai, Y., Hande, M.P., Matsumoto, T., Takehara, S., Tachibana, M., Oshimura, M., Lansdorp, P.M., and Furuichi, Y. 2000. Telomere maintenance in telomerase-deficient mouse embryonic stem cells: Characterization of an amplified telomeric DNA. *Mol. Cell. Biol.* **20:** 4115–4127.

O'Driscoll, M., Cerosaletti, K.M., Girard, P.M., Dai, Y., Stumm, M., Kysela, B., Hirsch, B., Gennery, A., Palmer, S.E., Seidel, J., et al. 2001. DNA ligase IV mutations identified in patients exhibiting developmental delay and immunodeficiency. *Mol. Cell* **8:** 1175–1185.

O'Hagan, R., Chang, S., Maser, R., Mohan, R., Artandi, S., Chin, L., and DePinho, R. 2002. Telomere dysfunction provokes regional amplification and deletion in cancer genomes. *Cancer Cell* **2:** 149.

Perrem, K., Bryan, T.M., Englezou, A., Hackl, T., Moy, E.L., and Reddel, R.R. 1999. Repression of an alternative mechanism for lengthening of telomeres in somatic cell hybrids. *Oncogene* **18:** 3383–3390.

Perrem, K., Colgin, L.M., Neumann, A.A., Yeager, T.R., and Reddel, R.R. 2001. Coexistence of alternative lengthening of telomeres and telomerase in hTERT-transfected GM847 cells. *Mol. Cell. Biol.* **21:** 3862–3875.

Rudolph, K.L., Chang, S., Lee, H.W., Blasco, M., Gottlieb, G.J., Greider, C., and DePinho, R.A. 1999. Longevity, stress response, and cancer in aging telomerase-deficient mice. *Cell* **96:** 701–712.

Rudolph, K.L., Chang, S., Millard, M., Schreiber-Agus, N., and DePinho, R.A. 2000. Inhibition of experimental liver cirrhosis in mice by telomerase gene delivery. *Science* **287:** 1253–1258.

Saito, Y., Kosugi, S., Suda, T., Wakabayashi, Y., Mishima, Y., Hatakeyama, K., and Kominami, R. 1997. Telomerase activity and metastasis: Expansion of cells having higher telomerase activity within culture lines and tumor tissues. *Jpn. J. Cancer Res.* **88:** 732–737.

Samper, E., Flores, J.M., and Blasco, M.A. 2001. Restoration of telomerase activity rescues chromosomal instability and premature aging in $Terc^{-/-}$ mice with short telomeres. *EMBO Rep.* **2:** 800–807.

Shay, J.W. and Bacchetti, S. 1997. A survey of telomerase activity in human cancer. *Eur. J. Cancer* **33:** 787–791.

Shay, J.W., Pereira-Smith, O.M., and Wright, W.E. 1991. A role for both RB and p53 in the regulation of human cellular senescence. *Exp. Cell Res.* **196:** 33–39.

Shay, J.W., Van Der Haegen, B.A., Ying, Y., and Wright, W.E. 1993. The frequency of immortalization of human fibroblasts and mammary epithelial cells transfected with SV40 large T-antigen. *Exp. Cell Res.* **209:** 45–52.

Shen, C.Y., Yu, J.C., Lo, Y.L., Kuo, C.H., Yue, C.T., Jou, Y.S., Huang, C.S., Lung, J.C., and Wu, C.W. 2000. Genome-wide search for loss of heterozygosity using laser capture microdissected tissue of breast carcinoma: An implication for mutator phenotype and breast cancer pathogenesis. *Cancer Res.* **60:** 3884–3892.

Stackpole, C.W. 1981. Distinct lung-colonizing and lung-metastasizing cell populations in B16 mouse melanoma. *Nature* **289:** 798–800.

Stampfer, M.R., Garbe, J., Levine, G., Lichtsteiner, S., Vasserot, A.P., and Yaswen, P. 2001. Expression of the telomerase catalytic subunit, hTERT, induces resistance to transforming growth factor β growth inhibition in p16INK4A$^-$ human mammary epithelial cells. *Proc. Natl. Acad. Sci.* **98:** 4498–503.

Stewart, S.A., Hahn, W.C., O'Connor, B.F., Banner, E.N., Lundberg, A.S., Modha, P., Mizuno, H., Brooks, M.W., Fleming, M., Zimonjic, D.B., et al. 2002. Telomerase contributes to tumorigenesis by a telomere length-independent mechanism. *Proc. Natl. Acad. Sci .USA.* **99:** 12606–12611.

Tang, R., Cheng, A.J., Wang, J.Y., and Wang, T.C. 1998. Close correlation between telomerase expression and adenomatous polyp progression in multistep colorectal carcinogenesis. *Cancer Res.* **58:** 4052–4054.

Todaro, G.J. and Green, H. 1963. Quantitative studies of the growth of mouse embryo cells in culture and their development into established lines. *J. Cell Biol.* **17:** 299–313.

Vaziri, H. and Benchimol, S. 1998. Reconstitution of telomerase activity in normal human cells leads to elongation of telomeres and extended replicative life span. *Curr. Biol.* **8:** 279–282.

Wright, W.E. and Shay, J.W. 1992. The two-stage mechanism controlling cellular senescence and immortalization. *Exp. Gerontol.* **27:** 383–389.

Wu, G., Lee, W.H., and Chen, P.L. 2000. NBS1 and TRF1 colocalize at promyelocytic leukemia bodies during late S/G_2 phases in immortalized telomerase-negative cells: Implication of NBS1 in alternative lengthening of telomeres. *J. Biol. Chem.* **275:** 30618–30622

Yan, P., Coindre, J.M., Benhattar, J., Bosman, F.T., and Guillou, L. 1999. Telomerase activity and human telomerase reverse transcriptase mRNA expression in soft tissue tumors: Correlation with grade, histology, and proliferative activity. *Cancer Res.* **59:** 3166–3170.

Yeager, T.R., Neumann, A.A., Englezou, A., Huschtscha, L.I., Noble, J.R., and Reddel, R.R. 1999. Telomerase-negative immortalized human cells contain a novel type of promyelocytic leukemia (PML) body. *Cancer Res.* **59:** 4175–4179.

Zhang, X., Mar, V., Zhou, W., Harrington, L., and Robinson, M.O. 1999. Telomere shortening and apoptosis in telomerase-inhibited human tumor cells. *Genes & Dev.* **13:** 2388–2399.

Zhu, C., Mills, K.D., Ferguson, D.O., Lee, C., Manis, J., Fleming, J., Gao, Y., Morton, C.C., and Alt, F.W. 2002. Unrepaired DNA breaks in p53-deficient cells lead to oncogenic gene amplification subsequent to translocations. *Cell* **109:** 811–821.